

See discussions, stats, and author profiles for this publication at: <https://www.researchgate.net/publication/354998709>

Adaptive Continuous Barrier Function Terminal Sliding Mode Control Technique for Disturbed Robotic Manipulator

Article in Circuits and Systems I: Regular Papers, IEEE Transactions on · October 2021

DOI: 10.1109/TCSI.2021.3101736

CITATIONS

27

READS

379

3 authors, including:



Saleh Mobayen

281 PUBLICATIONS 5,924 CITATIONS

SEE PROFILE



Khalid Alattas

University of Jeddah

53 PUBLICATIONS 277 CITATIONS

SEE PROFILE

Some of the authors of this publication are also working on these related projects:



Secure Communication in Wireless Sensor Networks Based on Chaos Synchronization [View project](#)



Design of a Global Sliding Mode Controller Using Hyperbolic Functions for Nonlinear Systems and Application in Chaotic Systems [View project](#)

Adaptive Continuous Barrier Function Terminal Sliding Mode Control Technique for Disturbed Robotic Manipulator

Published in: *IEEE Transactions on Circuits and Systems I: Regular Papers* (Volume: 68 , Issue: 10, Oct. 2021)

Page(s): 4403 - 4412

DOI: 10.1109/TCSI.2021.3101736

Date of Publication: 06 August 2021

Publisher: IEEE

► ISSN Information:

Saleh Mobayen, *Senior Member, IEEE*, Khalid A Alattas, *Member, IEEE*, Wudhichai Assawinchaichote

Abstract— This paper offers an improved finite time sliding mode controller scheme for a class of robotic manipulators with external disturbances. Since conventional sliding mode controllers have a discontinuous signum function, an important problem called chattering phenomenon can occur in them. The proposed scheme presents a new Lyapunov candidate functional containing an absolute function based on a fractional power of the switching surface such that the designed control law is continuous and smooth. The recommended control technique is designed using the Lyapunov stability theory and satisfies the presence of the sliding mode around designed switching surface in the finite time. The presented method eliminates the chattering problem produced by the switching controller and satisfies high precision action. Besides, the adaptive tuning controllers are designed to approximate the unknown bound of external disturbance. An extension of the proposed control technique based on the barrier function adaptive terminal sliding mode control is also suggested for better performance and robust tracking control of the nonlinear systems with external disturbances. Some simulation and experimental outcomes exhibit the efficacy of the planned technique.

Index Terms— Robotic manipulator; continuous sliding mode control; chattering phenomenon; second-order dynamics; finite time convergence.

I. INTRODUCTION

The classical Sliding Mode Control (SMC) technique has been provided to be an operative and robust control procedure for stabilization/tracking of various nonlinear processes in the existence of perturbations. The chief advantages of sliding mode control are the robustness versus uncertainty, rapid response, computational easiness, insensitivity to disturbance, and acceptable transient efficiency [1, 2]. For this purpose, the SMC approach has formed a great consideration of industrial and academic societies in the previous years. This method has been extensively applied in nearly all aspects of engineering, for example, civil, chemical, mechanics, robotics, electrical, and interdisciplinary engineering [3]. Specifically, in recent years, SMC has been broadly employed for the control/tracking of robotic manipulators [4-6]. The SMC approach has two principle phases: sliding phase and reaching phase. In this method, by employing a nonlinear control law, SMC changes the system dynamics and excites it to reach a pre-defined switching manifold in finite time [7]. The classical SMC procedure is based on definition of

the exponentially stable switching surface as a function of the state trajectories and employment of the Lyapunov stability theory to guarantee all states reach this curve in finite time.

The concepts of asymptotic and exponential stabilization present the reachability of the states to equilibrium over the infinite horizon [8]. However, in some applications such as bipedal locomotion, sampled-data systems, robotic manipulators, attitude control, aero-elastic systems, hypersonic vehicles, and other time-sensitive tasks, it is required to force the state responses to converge the stable equilibria in finite time. In recent years, the nonlinear Terminal Sliding Mode Control (TSMC) scheme has been planned, which makes the states to converge to zero in the finite time. TSMC offers superior characteristics, for instance, finite-time stability, low steady-state error and fast dynamic performance. Due to the mentioned superior characteristics, TSMC has been extensively employed in numerous applications such as robot manipulators, wheeled mobile robots, actuated exoskeleton, ship autopilot systems, multi-robot networks, nonholonomic systems and other robotic systems [9]. Both SMC and TSMC suffer from the unwanted oscillations called chattering problem. These oscillations are built via discontinuous control input which have sign functions and are destructive to practical actuators. The chattering phenomenon often exists in various types of the SMC. There are several techniques to eliminate the chattering problem in SMC, such as High-Order Sliding-Mode (HOSM) approach [10], boundary layer scheme [11] and disturbance estimation technique [12]. The boundary layer approach comprises the saturation and sigmoid functions. The main influence of HOSM is that the discontinuous sign function is available in time-derivative of controller signal; thus, the actual control input originated by integration is a continuous signal which can remove the chattering phenomenon. HOSM typically allows the reduction of the chattering effect while providing the convergence to surface in finite time. In the systems with parameter uncertainty and exterior disturbance which are immeasurable in practice, a disturbance estimation procedure is required. Actually, one main issue in the design process of SMC is the necessity of the perturbations bounds which are used in the switching control law.

In [13], an adaptive TSMC technique is suggested for nonlinear differential inclusion systems with external disturbance. In [14], a

S. Mobayen is with Future Technology Research Center, National Yunlin University of Science and Technology, Douliou, Yunlin 64002, Taiwan (Email: mobayens@yuntech.edu.tw). K.A. Alattas is with Department of Computer Science and Artificial Intelligence, College of Computer Science and Engineering, University of

Jeddah, Jeddah, Saudi Arabia (Email: kaalattas@uj.edu.sa). W. Assawinchaichote is with Department of Electronic and Telecommunication Engineering, Faculty of Engineering, King Mongkut's University of Technology Thonburi, Bangkok 10140, Thailand (Email: wudhichai.asa@kmutt.ac.th).

second-order adaptive TSMC approach is offered for stabilization of a two-link robotic manipulator. An adaptive decentralized attitude synchronization control based on nonsingular fast TSMC for spacecraft formation is designed in [15]. An adaptive fast TSMC scheme combined with the Global Sliding Mode Control (GSMC) is presented in [16] for tracking control of nonlinear systems with uncertainties. Reference [17] proposes an adaptive nonsingular TSMC for finite time tracking of a gyroscope of Micro-Electro-Mechanical System (MEMS) in the existence of parameter variations and high-amplitude perturbations. In [18], the TSMC scheme is planned for a hypersonic vehicle via a disturbance observer. In [19], a continuous adaptive fast TSMC method is planned for tracking of the position of robotic manipulators. Reference [20] proposes an adaptive robust TSMC approach for near-space vehicles via Second-Order Sliding Mode (SOSM). A novel fast nonsingular TSMC is investigated in [21] to plan the terminal angle constraint guidance for interception of the maneuvering target with command chattering reduction in the guidance law. In [22], a nonsingular chattering-free TSMC technique based on super-twisting is planned for attitude tracking of a quad-rotor. In [23], in the light of the nonlinear disturbance observer, an adaptive TSMC method is recommended for hypersonic flight vehicles. An adaptive TSMC approach with projection operator is recommended in [24] for tracking control of hybrid energy storage system. A nonlinear disturbance-observer-based adaptive TSMC approach is proposed in [25], which is employed to stabilize the reentry vehicle attitude. In [26], an adaptive high-order TSMC with delay estimation is suggested for robot manipulator in the existence of backlash hysteresis. An adaptive nonsingular fractional order super-twisting TSMC based on delay estimation is planned in [27] for cable-driven manipulators. In [28], a nonsingular adaptive fractional-order TSMC with delay estimation is designed for the high-precision tracking of cable-driven manipulators in the existence of lumped uncertainty. In [29], a robust non-singular adaptive TSMC based on dynamic inversion is designed for position / attitude tracking of a practical quadrotor. References [30] proposes an adaptive observer-based composite TSMC for the stability of uncertain nonlinear dynamical systems. A delay-estimation-based adaptive super-twisting nonsingular fast TSMC technique is presented in [31] to satisfy the high-precise tracking of uncertain cable-driven manipulator. In [32], using a neural dynamic manifold, an adaptive integral TSMC technique is proposed for robust tracking of fully-actuated mechanical systems. In [33], an adaptive back-stepping integral fast TSMC is planned for the finite time tracking control of quadrotor vehicles, where some parameter-tuning laws are designed for estimation of mass and inertia moment of quadrotor, and compensation of unknown bounds of external disturbances. In [34], an adaptive continuous-twisting control method is proposed for the double-integrator with a Lipschitz continuous perturbation, which assures the states convergence to the origin in the finite time. Two output feedback controllers based on the continuous-twisting algorithm are designed in [35], where the proposed state observers are based on the first and second order robust exact differentiators. In [36], the continuous integral super-twisting SMC approach is proposed for linear and nonlinear systems with matched disturbances, substituting the discontinuous term of feedback controller by a super-twisting law. However, none of the researches [34-36] have been focused on the adaptive barrier-function-based TSMC approach for development of robust tracking control of nonlinear perturbed systems. All the methodologies presented in the above-stated works stimulate investigators to establish the suggested technique of the proposed article. To the highest of the author's familiarity, very little endeavors have been done to propose an adaptive robust TSMC approach which can eliminate discontinuity in the control laws. In this paper, we propose yet another technique to avoid chattering phenomenon in TSMC, which is the main drawback of SMC and TSMC. We incorporate the notions of finite time stability and disturbance observer to attain finite time tracker for robotic manipulators with the nonlinear

second-order structure and external disturbances. The planned control approach proposes a novel Lyapunov candidate function including a fractional-power absolute function of the switching surface, where the designed controller is continuous and smooth. This technique removes the chattering phenomenon created via the switching law and guarantees the high precision efficiency. A parameter-tuning adaptive control scheme is designed to guessimate the unknown bound of disturbance.

This article is presented as the following layout: the problem formulation for the robotic manipulators is presented in Sect. 2. In Sect. 3, main results containing the novel Lyapunov candidate function with an absolute term and two adaptive finite time (discontinuous/continuous) controllers are proposed. In Sect. 4, the simulation and experimental outcomes are provided and finally, conclusions are specified in Sect. 5.

II. PROBLEM DESCRIPTION

Consider the Euler-Lagrange dynamical equation of the robotic manipulators as

$$B_0(q(t), \dot{q}(t))\ddot{q}(t) + C_0(q(t), \dot{q}(t))\dot{q}(t) + G_0(q(t)) = u(t), \quad (1)$$

where $q(t)$, $\dot{q}(t)$, $\ddot{q}(t)$ indicate the joint position, joint velocity and joint acceleration, correspondingly; $u(t)$ signifies the control vector indicating the torque employed on the joints; $B_0(q(t), \dot{q}(t))$ signifies the inertia matrix; $C_0(q(t), \dot{q}(t))$ represents the centripetal Coriolis matrix; $G_0(q(t))$ shows the gravity vector. The dynamical equation (1) are denoted in second-order form with disturbance as

$$\ddot{x}_i(t) = g_i(x_i(t), \dot{x}_i(t)) + h_i(x_i(t), \dot{x}_i(t))u_i(t) + d_i(x_i(t), t), \quad (2)$$

where $x_i \in R$ signifies the states (joint positions) of robotic manipulator, $u_i(t) \in R$ signifies the controller signal, $g_i(x_i(t), \dot{x}_i(t))$ and $h_i(x_i(t), \dot{x}_i(t)) \neq 0$ represent two known functions, and $d_i(x_i(t), t)$ indicates the unknown disturbance but bounded as $|d_i(x_i(t), t)| < D_i$.

Assumption 1: The states $x_i(t)$ and $\dot{x}_i(t)$ are available as measured outputs, then, the relative degree is one over $\dot{x}_i(t) \neq 0$.

The second-order robotic manipulator (2) is assumed to track the desired reference $x_{d_i}(t)$. The error signal is formed as

$$\tilde{x}_i(t) = x_i(t) - x_{d_i}(t). \quad (3)$$

Let us consider the sliding surface expressed as follow:

$$s_i(t) = \dot{\tilde{x}}_i(t) + \lambda_i \tilde{x}_i(t), \quad (4)$$

where the constant parameter λ_i should be positive to satisfy the closed-loop stability when the states reach the switching surface.

Lemma 1 [37]: Let $x \in \mathfrak{N} \subset R^n$, $\dot{x} = \mathfrak{F}(x)$, $\mathfrak{F}: R^n \rightarrow R^n$ is a continuous function on an open neighborhood \mathfrak{N} of the origin and locally Lipschitz on $\mathfrak{N} \setminus \{0\}$ and $\mathfrak{F}(0) = 0$. Assume there is a continuous function $V: \mathfrak{N} \rightarrow R$ where (a) V is positive-definite; (b) \dot{V} is negative on $\mathfrak{N} \setminus \{0\}$; (c) there exist real-positive values m and $0 < \alpha < 1$, and a neighborhood $N \subset \mathfrak{N}$ of the origin where

$$\dot{V} + mV^\alpha \leq 0 \quad (5)$$

on $N \setminus \{0\}$. So, the origin is finite-time stable for system $\dot{x} = \mathfrak{F}(x)$.

Then, for the initial time t_0 , the Lyapunov functional reaches zero in finite time as

$$t_s = t_0 + \frac{V^{1-\alpha}(t_0)}{c(1-\alpha)} \quad (6)$$

where t_s is the settling time.

III. MAIN RESULTS

In what follows, a novel technique defining a Lyapunov candidate function with an absolute term is proposed as a solution to feature a continuous and smooth adaptive control law in the sliding approach. The main objective of the new continuous SMC scheme is to design a controller such that the chattering problem is removed. In this work, the subsequent control law is planned for the robotic manipulator (2):

$$u_i(t) = h_i(x_i(t), \dot{x}_i(t))^{-1} \left(\ddot{x}_{di}(t) - \frac{\mu_i n}{\eta_i m} s_i(t)^{b+1-\frac{m}{n}} - \lambda_i \dot{x}_i(t) - g_i(x_i(t), \dot{x}_i(t)) \right) \quad (7)$$

where η_i and μ_i indicate two positive constants to adjust the speed of the reaching to the sliding surface; m and n specify two positive odd integers with $m > n$; b is a positive odd integer.

To verify the stability of the robotic manipulator (2) under the controller (7), we define the novel Lyapunov candidate function as

$$\begin{aligned} V_i(t) &= \eta_i |s_i(t)|^{\frac{m}{n}} \\ &= \eta_i s_i(t)^{\frac{m}{n}} \operatorname{sgn}(s_i(t)^{\frac{m}{n}}) \\ &= \eta_i s_i(t)^{\frac{m}{n}} \operatorname{sgn}(s_i(t)). \end{aligned} \quad (8)$$

Taking the time derivative of Lyapunov function (8), one obtains

$$\dot{V}_i(t) = \eta_i \frac{m}{n} s_i(t)^{\frac{m}{n}-1} \dot{s}_i(t) \operatorname{sgn}(s_i(t)). \quad (9)$$

In order to satisfy the stabilization of the robotic manipulator (2), the differentiation of the Lyapunov function (8) must be negative. Hence, for $\dot{V}_i(t) < 0$, one has

$$\begin{aligned} \dot{V}_i(t) &= -\mu_i |s_i(t)|^b \\ &= -\mu_i s_i(t)^b \operatorname{sgn}(s_i(t)) < 0, \end{aligned} \quad (10)$$

where using (9) and (10), we have

$$\dot{s}_i(t) = -\frac{\mu_i n}{\eta_i m} s_i(t)^{b+1-\frac{m}{n}}. \quad (11)$$

Substituting the time-derivative of switching surface (4) into (11) leads to

$$\ddot{x}_i(t) + \lambda_i \dot{x}_i(t) = -\frac{\mu_i n}{\eta_i m} s_i(t)^{b+1-\frac{m}{n}}. \quad (12)$$

Then, using (2), (3) and (12), the equivalent controller is obtained as (7). Now, substituting (7) into (9), one obtains

$$\begin{aligned} \dot{V}_i(t) &= \eta_i \frac{m}{n} s_i(t)^{\frac{m}{n}-1} \operatorname{sgn}(s_i(t)) \left(d_i(x_i(t), t) \right. \\ &\quad \left. - \frac{\mu_i n}{\eta_i m} s_i(t)^{b+1-\frac{m}{n}} \right) \end{aligned} \quad (13)$$

where because $s_i(t)^{\frac{m}{n}-1} \operatorname{sgn}(s_i(t)) > 0$ and $\dot{V}_i(t) < 0$ (for guarantying the stability), the following condition must be fulfilled:

$$d_i(x_i(t), t) - \frac{\mu_i n}{\eta_i m} s_i(t)^{b+1-\frac{m}{n}} \leq 0 \quad (14)$$

or equivalently

$$\mu_i \geq \frac{\eta_i m D_i}{n} s_i(t)^{\frac{m}{n}-b-1}. \quad (15)$$

Eq. (15) satisfies the robust stability of the robotic manipulator dynamics (2).

The upper bounds of external disturbance are unknown practically and hence, it is hard to find a suitable parameter D_i . In what follows, two adaptive finite time (discontinuous/continuous) controllers are presented to approximate the unknown upper bound of disturbance.

Theorem 1: Consider the robotic manipulator (2) and sliding surface (4). Assume that disturbance $d_i(x_i(t), t)$ is unknown but bounded with $|d_i(x_i(t), t)| < D_i$. Suppose $\tilde{D}_i(t)$ as estimation of D_i which is adapted as

$$\dot{\tilde{D}}_i = \psi_i |s_i(t)|, \quad (16)$$

where $\psi_i > 0$. Using the adaptive controller as

$$u_i(t) = h_i(x_i(t), \dot{x}_i(t))^{-1} \left(\ddot{x}_{di}(t) - g_i(x_i(t), \dot{x}_i(t)) - \tilde{D}_i(t) \operatorname{sgn}(s_i(t)) - \lambda_i \dot{x}_i(t) \right) \quad (17)$$

then, the state trajectories of robotic manipulator (2) are converged to switching surface (4) in finite time.

Proof: Consider positive-definite Lyapunov functional is described as

$$V_i(t) = 0.5 \mu_i \tilde{D}_i(t)^2 + 0.5 s_i(t)^2, \quad (18)$$

where $\tilde{D}_i(t) = \hat{D}_i(t) - D_i$ and μ_i is a scalar with $0 < \mu_i < \psi_i^{-1}$. Differentiating (18) with respect to time and using (4) and (16), we find

$$\begin{aligned} \dot{V}_i(t) &= \mu_i \tilde{D}_i(t) \dot{\tilde{D}}_i(t) + s_i(t) \dot{s}_i(t) \\ &= \mu_i \psi_i \tilde{D}_i(t) |s_i(t)| + s_i(t) (\ddot{x}_i(t) + \lambda_i \dot{x}_i(t)). \end{aligned} \quad (19)$$

From (2) and (3), it follows from (19) that

$$\begin{aligned} \dot{V}_i(t) &= \mu_i \psi_i \tilde{D}_i(t) |s_i(t)| + s_i(t) (g_i(x_i(t), \dot{x}_i(t)) \\ &\quad + h_i(x_i(t), \dot{x}_i(t)) u_i(t) + d_i(x_i(t), t) + \lambda_i \dot{x}_i(t) - \ddot{x}_{di}(t)), \end{aligned} \quad (20)$$

where substituting (17) into (20) yields

$$\begin{aligned} \dot{V}_i(t) &= \mu_i \psi_i \tilde{D}_i(t) |s_i(t)| \\ &\quad + s_i(t) (d_i(x_i(t), t) - \tilde{D}_i(t) \operatorname{sgn}(s_i(t))) \\ &\leq \mu_i \psi_i \tilde{D}_i(t) |s_i(t)| + |s_i(t)| |d_i(x_i(t), t)| \\ &\quad - \tilde{D}_i(t) |s_i(t)| + D_i |s_i(t)| - D_i |s_i(t)| \\ &\leq -(1 - \mu_i \psi_i) \tilde{D}_i(t) |s_i(t)| - (D_i - |d_i(x_i(t), t)|) |s_i(t)| \end{aligned} \quad (21)$$

Since $D_i > |d_i(x_i(t), t)|$ and $\mu_i \psi_i < 1$, hence, Eq. (21) is expressed as

$$\begin{aligned} \dot{V}_i(t) &\leq -\sqrt{2} (D_i - |d_i(x_i(t), t)|) \frac{|s_i|}{\sqrt{2}} \\ &\quad - \sqrt{\frac{2}{\mu_i}} (1 - \mu_i \psi_i) |s_i| \sqrt{\frac{\mu_i}{2}} \tilde{D}_i \\ &\leq -\min \left\{ \sqrt{2} (D_i - |d_i(x_i(t), t)|), \sqrt{\frac{2}{\mu_i}} (1 - \mu_i \psi_i) \right. \\ &\quad \left. - \mu_i \psi_i |s_i(t)| \right\} \left(\frac{|s_i(t)|}{\sqrt{2}} + \sqrt{\frac{\mu_i}{2}} \tilde{D}_i(t) \right) \\ &= -\Xi_i V_i(t)^{0.5}, \end{aligned} \quad (22)$$

where $\Xi_i = \min \left\{ \sqrt{2} (D_i - |d_i(x_i(t), t)|), \sqrt{\frac{2}{\mu_i}} (1 - \mu_i \psi_i) |s_i(t)| \right\} > 0$. In conclusion, according to Lemma 1, via the adaptive controller (17), the trajectories of robotic manipulator (2) reach the sliding surface in the finite time. \square

Theorem 2: Consider the robotic system described by the nonlinear second-order equation (2) and the proportional-derivative sliding surface (4). Suppose that the external disturbance $d_i(x(t), t)$ is unknown and bounded, where $D_i > 0$ is unknown scalar. Assume that $\hat{D}_i(t)$ is the estimate of D_i with the following adaptation law:

$$\dot{\hat{D}}_i(t) = \psi_i |s_i(t)|^{\frac{m}{n}-1}, \quad (23)$$

where $\psi_i > 0$. Employing the adaptive controller as

$$u_i(t) = h_i(x_i(t), \dot{x}_i(t))^{-1} \left(\ddot{x}_{di}(t) - \frac{\mu_i n}{\eta_i m} s_i^{b+1-\frac{m}{n}} - g_i(x_i(t), \dot{x}_i(t)) - \lambda_i \dot{x}_i(t) - \widehat{D}_i(t) \right) \quad (24)$$

then the finite time convergence of state trajectories to the surface (4) is fulfilled.

Proof: The new Lyapunov function is defined as

$$V_i(t) = \eta_i s_i(t)^{\frac{m}{n}} \text{sgn}(s_i(t)) + 0.5 \ell_i \widehat{D}_i(t)^2, \quad (25)$$

where $\widehat{D}_i(t) = \widehat{D}_i(t) - D_i$ and $0 < \ell_i < \frac{\eta_i m}{\psi_i n}$. Differentiating Eq. (25), and using (4) and (23) yields

$$\begin{aligned} \dot{V}_i(t) &= \frac{\eta_i m}{n} s_i(t)^{\frac{m}{n}-1} \dot{s}_i(t) \text{sgn}(s_i(t)) + \ell_i \widehat{D}_i(t) \dot{\widehat{D}}_i(t) \\ &= \frac{\eta_i m}{n} s_i(t)^{\frac{m}{n}-1} (\ddot{x}_i(t) + \lambda_i \dot{x}_i(t)) \text{sgn}(s_i(t)) \\ &\quad + \ell_i \psi_i \widehat{D}_i(t) |s_i(t)|^{\frac{m}{n}-1}. \end{aligned} \quad (26)$$

From (2) and (3), Eq. (26) is written as

$$\begin{aligned} \dot{V}_i(t) &= \ell_i \psi_i (\widehat{D}_i(t) - D_i) |s_i(t)|^{\frac{m}{n}-1} \\ &\quad + \frac{\eta_i m}{n} s_i(t)^{\frac{m}{n}-1} (g_i(x_i(t), \dot{x}_i(t)) \\ &\quad + h_i(x_i(t), \dot{x}_i(t)) u_i(t) + d_i(x_i(t), t) + \lambda_i \dot{x}_i(t) \\ &\quad - \ddot{x}_{di}(t)) \text{sgn}(s_i(t)) \end{aligned} \quad (27)$$

where substituting (24) into (27) leads to

$$\begin{aligned} \dot{V}_i(t) &= \ell_i \psi_i (\widehat{D}_i(t) - D_i) |s_i(t)|^{\frac{m}{n}-1} - \mu_i |s_i(t)|^b \\ &\quad - \frac{\eta_i m}{n} \widehat{D}_i(t) |s_i(t)|^{\frac{m}{n}-1} + \frac{\eta_i m}{n} d_i(x_i(t), t) |s_i(t)|^{\frac{m}{n}-1}. \end{aligned} \quad (28)$$

Eq. (28) can be rewritten as

$$\begin{aligned} \dot{V}_i &\leq \ell_i \psi_i \widehat{D}_i(t) |s_i(t)|^{\frac{m}{n}-1} - \frac{\eta_i m}{n} \widehat{D}_i(t) |s_i(t)|^{\frac{m}{n}-1} \\ &\quad + \frac{\eta_i m}{n} |d_i(x_i(t), t)| |s_i(t)|^{\frac{m}{n}-1} + \frac{\eta_i m}{n} (D_i - D_i) |s_i(t)|^{\frac{m}{n}-1} \\ &\leq -\frac{\eta_i m}{n} (D_i - |d_i(x_i(t), t)|) |s_i(t)|^{\frac{m}{n}-1} \\ &\quad - \left(\frac{\eta_i m}{n} - \ell_i \psi_i \right) \widehat{D}_i(t) |s_i(t)|^{\frac{m}{n}-1}. \end{aligned} \quad (29)$$

Since $D_i > |d_i(x_i(t), t)|$ and $\ell_i \psi_i < \frac{\eta_i m}{n}$, then, we have

$$\begin{aligned} \dot{V}_i &\leq -\frac{m\sqrt{\eta_i}}{n} (D_i - |d_i(x_i(t), t)|) |s_i(t)|^{\frac{m}{2n}-1} \left(\sqrt{\eta_i} |s_i(t)|^{\frac{m}{2n}} \right) \\ &\quad - \sqrt{\frac{2}{\ell_i}} \left(\frac{\eta_i m}{n} \right) \\ &\quad - \ell_i \psi_i |s_i(t)|^{\frac{m}{n}-1} \left(\sqrt{\frac{\ell_i}{2}} \widehat{D}_i(t) \right) \\ &\leq -\min \left\{ \frac{m\sqrt{\eta_i}}{n} (D_i - |d_i(x_i(t), t)|) |s_i(t)|^{\frac{m}{2n}-1} \right. \\ &\quad \left. , \sqrt{\frac{2}{\ell_i}} \left(\frac{\eta_i m}{n} - \ell_i \psi_i \right) |s_i(t)|^{\frac{m}{n}-1} \right\} \left(\sqrt{\eta_i} |s_i(t)|^{\frac{m}{2n}} + \sqrt{\frac{\ell_i}{2}} \widehat{D}_i(t) \right) \\ &= -\Omega_i V_i(t)^{0.5}, \end{aligned} \quad (30)$$

where $\Omega_i = \min \left\{ \frac{m\sqrt{\eta_i}}{n} (D_i - |d_i(x_i(t), t)|) |s_i(t)|^{\frac{m}{2n}-1}, \sqrt{\frac{2}{\ell_i}} \left(\frac{\eta_i m}{n} - \ell_i \psi_i \right) |s_i(t)|^{\frac{m}{n}-1} \right\} > 0$. Finally, according to Lemma 1, using the adaptive controller (24), states of robotic manipulator (2) are converged to surface $s_i = 0$ in finite time. \square

Remark 1: As it can be observed from (24), the suggested control scheme gives insights for the elimination of the chattering phenomenon because no signum function is employed in (24). Hence,

the offered control law is continuous and smooth. The schematic diagram of the proposed control configuration is displayed in Fig.1.

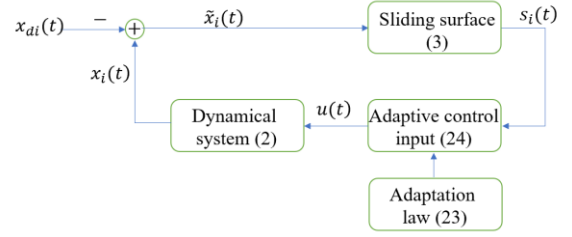


Fig.1. Schematic diagram of the proposed control method.

Remark 2: By some modifications, the proposed control technique can also be employed on n -dimensional nonlinear systems.

Remark 3: For the extension of the proposed control method, the barrier function-based adaptive terminal sliding mode control method is studied for the robust tracking control of the nonlinear second-order systems in the presence of external disturbances. Then, a new adaptive control law based on the barrier function is designed in this section. The external disturbances can be estimated by using the barrier-based adaptive TSMC more efficiently, and the closed-loop system becomes more stable. Using the control law (24) with

$$\widehat{D}_i(t) = \begin{cases} \widehat{D}_{i_a}(t), & \text{if } 0 < t \leq \bar{t} \\ \widehat{D}_{i_{psd}}(t), & \text{if } t > \bar{t} \end{cases} \quad (31)$$

where \bar{t} denotes the time that the error converges to the neighborhood ε of the surface $s(t)$. The adaptation law and the positive-semi-definite (PSD) barrier function are provided by

$$\widehat{D}_{i_a}(t) = \psi_i |s_i(t)|^{\frac{m}{n}-1} \quad (32)$$

$$\widehat{D}_{i_{psd}}(t) = \frac{|s_i(t)|}{\varepsilon_i - |s_i(t)|}, \quad (33)$$

where ε is a positive scalar. Using the adaptation law (32), the control gain is tuned to be increased until the error trajectories reach the neighborhood ε of the surface at time \bar{t} . For the times bigger than \bar{t} , the adaptation gain switches to the PSD barrier function which decreases the convergence region and maintains the error trajectories in that region. For the condition $0 < t \leq \bar{t}$, the controller design is proposed in Theorem 2. For the condition that the time is greater than \bar{t} ($t > \bar{t}$), the barrier-function-based adaptive controller is designed as

$$u_i(t) = h_i(x_i(t), \dot{x}_i(t))^{-1} \left(\ddot{x}_{di}(t) - g_i(x_i(t), \dot{x}_i(t)) - \lambda_i \dot{x}_i(t) - \widehat{D}_{i_{psd}}(t) \text{sgn}(s_i(t)) \right) \quad (34)$$

then the error trajectories reach the convergence region $|s_i(t)| \leq \varepsilon$ in the finite time.

Consider the Lyapunov candidate functional as

$$V_i(t) = 0.5 \left(s_i(t)^2 + (\widehat{D}_{i_{psd}}(t) - \widehat{D}_{i_{psd}}(0))^2 \right), \quad (35)$$

where using the time-derivate of the Lyapunov function (35), we have

$$\dot{V}_i(t) = s_i(t) \dot{s}_i(t) + (\widehat{D}_{i_{psd}}(t) - \widehat{D}_{i_{psd}}(0)) \dot{\widehat{D}}_{i_{psd}}(t), \quad (36)$$

where substituting $\dot{s}_i(t)$ and $\widehat{D}_{i_{psd}}(0) = 0$ in the above equation, we obtain

$$\begin{aligned} \dot{V}_i(t) &= s_i(t) (g_i(x_i(t), \dot{x}_i(t)) + h_i(x_i(t), \dot{x}_i(t)) u_i(t) + \\ &\quad d_i(x_i(t), t) + \lambda_i \dot{x}_i(t) - \ddot{x}_{di}(t)) + \widehat{D}_{i_{psd}}(t) \dot{\widehat{D}}_{i_{psd}}(t), \end{aligned} \quad (37)$$

Replacing the control input (34) into (37) yields

$$\begin{aligned}
 & \dot{V}_i(t) \\
 &= s_i(t) \left(-\widehat{D}_{i_psd}(t) \operatorname{sgn}(s_i(t)) + d_i(x_i(t), t) \right) \\
 &+ \widehat{D}_{i_psd}(t) \widehat{D}_{i_psd}(t) \\
 &\leq |s_i(t)| \left\{ |d_i(x_i(t), t)| - \widehat{D}_{i_psd}(t) \right\} + \widehat{D}_{i_psd}(t) \widehat{D}_{i_psd}(t) \\
 &\leq |s_i(t)| \left\{ |d_i(x_i(t), t)| - \widehat{D}_{i_psd}(t) \right\} \\
 &+ \widehat{D}_{i_psd}(t) \frac{\varepsilon}{(\varepsilon - |s_i(t)|)^2} \operatorname{sgn}(s_i(t)) \dot{s}_i(t) \\
 &\leq |s_i(t)| \left\{ |d_i(x_i(t), t)| - \widehat{D}_{i_psd}(t) \right\} \\
 &+ \widehat{D}_{i_psd}(t) \frac{\varepsilon}{(\varepsilon - |s_i(t)|)^2} [d_i(x_i(t), t) \\
 &- \widehat{D}_{i_psd}(t) \operatorname{sgn}(s_i(t))] \operatorname{sgn}(s_i(t))
 \end{aligned} \tag{38}$$

Equation (38) can be written as

$$\begin{aligned}
 \dot{V}_i(t) &\leq -\left\{ \widehat{D}_{i_psd}(t) - |d_i(x_i(t), t)| \right\} |s_i(t)| \\
 &\quad - \widehat{D}_{i_psd}(t) \frac{\varepsilon}{(\varepsilon - |s_i(t)|)^2} \left[\widehat{D}_{i_psd}(t) \right. \\
 &\quad \left. - |d_i(x_i(t), t)| \right]
 \end{aligned} \tag{39}$$

where since $\widehat{D}_{i_psd}(t) \geq |d_i(x_i(t), t)|$ and $\frac{\varepsilon}{(\varepsilon - |s_i(t)|)^2} > 0$, one finds

$$\begin{aligned}
 \dot{V}_i(t) &\leq -\sqrt{2} \left\{ \widehat{D}_{i_psd}(t) - |d_i(x_i(t), t)| \right\} \frac{|s_i(t)|}{\sqrt{2}} \\
 &\quad - \frac{\sqrt{2}\varepsilon}{(\varepsilon - |s_i(t)|)^2} \left[\widehat{D}_{i_psd}(t) \right. \\
 &\quad \left. - |d_i(x_i(t), t)| \right] \frac{\widehat{D}_{i_psd}(t)}{\sqrt{2}} \\
 &\leq -Z \left(\frac{|s_i(t)|}{\sqrt{2}} + \frac{\widehat{D}_{i_psd}(t)}{\sqrt{2}} \right) \leq -ZV_i(t)^{0.5}
 \end{aligned} \tag{40}$$

where $Z = \sqrt{2} \left\{ \widehat{D}_{i_psd}(t) - |d_i(x_i(t), t)| \right\} \min \left\{ 1, \frac{\sqrt{2}\varepsilon}{(\varepsilon - |s_i(t)|)^2} \right\}$. \square

IV. SIMULATION AND EXPERIMENTAL RESULTS

Example 1: Three degrees of freedom manipulator

In this part, the controller planned in Theorems 1 and 2 are employed on three-degrees of freedom manipulator displayed in Fig.2. In the case study, l_1, l_2, l_3 are distances of center of mass of three rigid links from joint axis, $m_{l_1}, m_{l_2}, m_{l_3}$ introduce the masses of links, $m_{m_1}, m_{m_2}, m_{m_3}$ indicate the rotors' masses, $I_{l_1}, I_{l_2}, I_{l_3}$ are inertia moments of the links, and $I_{m_1}, I_{m_2}, I_{m_3}$ are inertia moments of the rotors.

Consider the dynamic equations of three-degrees of freedom manipulator as

$$B_0 \ddot{q} + H_0 \dot{q} + F_{d\dot{q}} + F_{s\dot{q}} + T_0 + G_0 = u(t) \tag{41}$$

$$\text{with } B_0 = \begin{bmatrix} b_{11} & b_{12} & b_{13} \\ b_{21} & b_{22} & b_{23} \\ b_{31} & b_{32} & b_{33} \end{bmatrix}, H_0 = \begin{bmatrix} h_{11} & h_{12} & h_{13} \\ h_{21} & h_{22} & h_{23} \\ h_{31} & h_{32} & h_{33} \end{bmatrix}, F_{d\dot{q}} = \begin{bmatrix} f_d \dot{q}_1 \\ f_d \dot{q}_2 \\ f_d \dot{q}_3 \end{bmatrix},$$

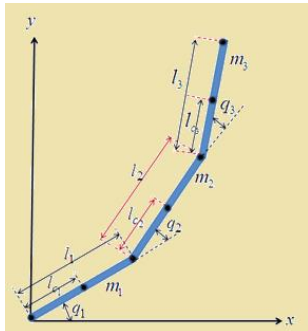


Fig.2. Three-degrees of freedom rigid manipulator.

$$F_{s\dot{q}} = \begin{bmatrix} f_s \operatorname{sgn}(\dot{q}_1) \\ f_s \operatorname{sgn}(\dot{q}_2) \\ f_s \operatorname{sgn}(\dot{q}_3) \end{bmatrix}, T_0 = \begin{bmatrix} \tau_1 \\ \tau_1 \\ \tau_1 \end{bmatrix} \text{ and } G_0 = \begin{bmatrix} g_1(q) \\ g_2(q) \\ g_3(q) \end{bmatrix}, \text{ where the system}$$

parameters are defined in Appendix 1. The parameters of the rigid manipulator and controller are given as $f_d = f_s = 5$, $l_1 = l_2 = l_3 = 0.5m$, $m_{l_1} = m_{l_2} = m_{l_3} = 10kg$, $m_{m_1} = m_{m_2} = m_{m_3} = 1kg$, $I_{l_1} = I_{l_2} = I_{l_3} = 1kg \cdot m^2$, $m = 5$, $a_1 = a_2 = 1$, $k_{r_1} = k_{r_2} = k_{r_3} = 1$, $I_{m_1} = I_{m_2} = I_{m_3} = 0.01kg \cdot m^2$, $\mu_1 = \mu_2 = \mu_3 = 0.4$, $n = 3, \tau_1 = 10(1 + \cos(0.5\pi t) + \sin(2t) + \sin(1.5t) + \sin(0.5\pi t)), \lambda = 8$. The initial condition is given as $q(0) = [-2 \ -1 \ 5]^T$. The desired trajectory is specified as $q_d = [2 \sin(t) + 1, 2 \sin(t) - 3, 8 \sin(t)]^T$. Comparing the dynamical equations (2) and (41), we obtain $x(t) = q$, $\dot{x}(t) = \dot{q}$, $\ddot{x}(t) = \ddot{q}$, $h(x(t), \dot{x}(t)) = -B_0^{-1} \{H_0 \dot{q} + F_{d\dot{q}} + F_{s\dot{q}}\}$, $h(x(t), \dot{x}(t)) = B_0^{-1}$ and $d(x(t), t) = -B_0^{-1} \{T_0 + G_0\}$.

The proposed adaptive parameter-tuning control law is designed as (24). Time histories of position of joints are displayed in Fig.3. It is exhibited from this figure that the states of position track the reference trajectories, suitably. Time responses of switching surfaces are displayed in Fig.4, exhibiting that the surface is chattering-free. Fig.5 illustrates time response of controller signals and time responses of adaptation gains are demonstrated in Fig.6. It can be observed from Fig.5 that the proposed control signals have suitable amplitude and they have no high-frequency oscillations. Moreover, as can be confirmed from Fig.6, since the time-derivative of \widehat{D}_i is in the form of an absolute term, the estimation of the external disturbance has a slight slope, which is negligible in the results (also for longer time). The final values of the adaptation gains are found as $\widehat{D} = [0.4338, 0.9665, 0.4142]^T$. This simulation shows the feasibility and effectiveness of the suggested scheme.

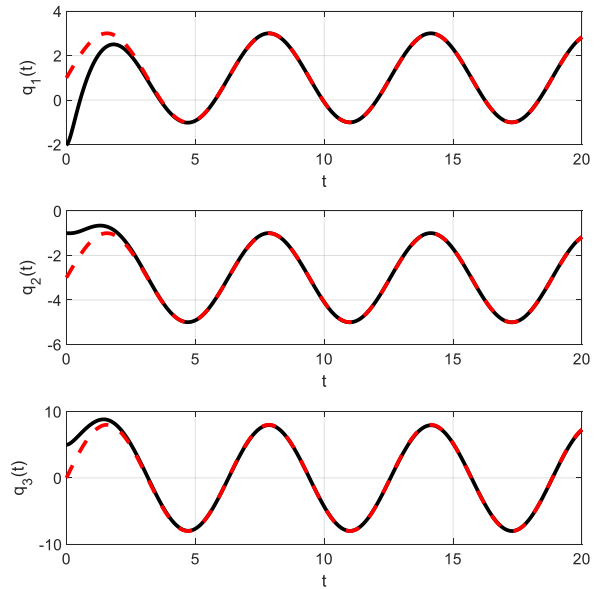


Fig.3. Time histories of position of joints (reference signals—red dashed red line, actual signals—black solid line).

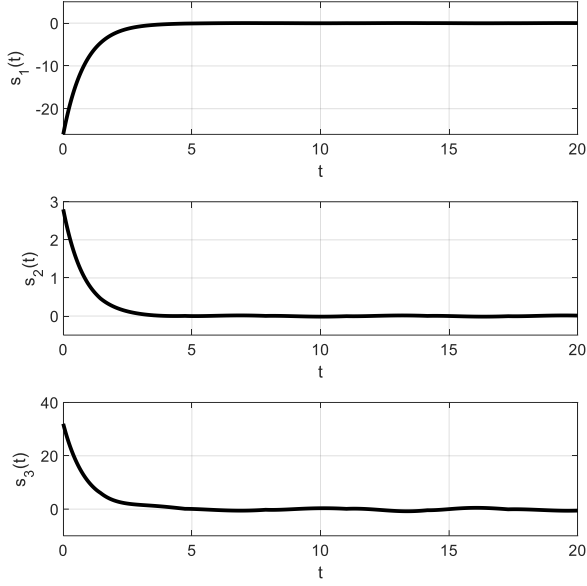


Fig.4. Sliding surfaces.

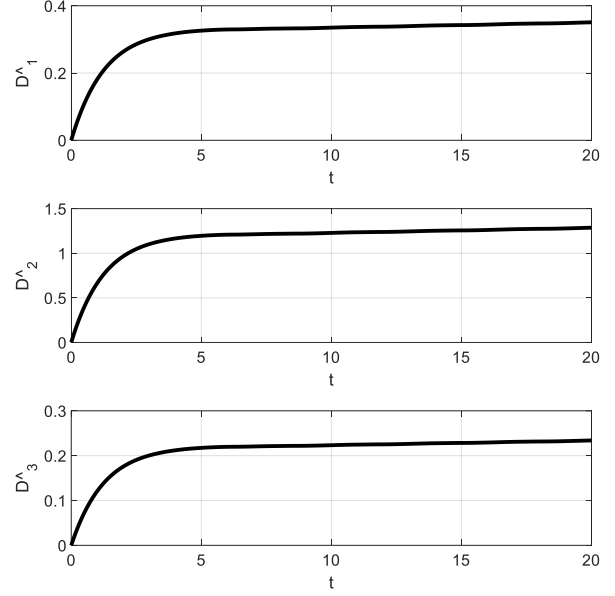


Fig.6. Adaptation gains.

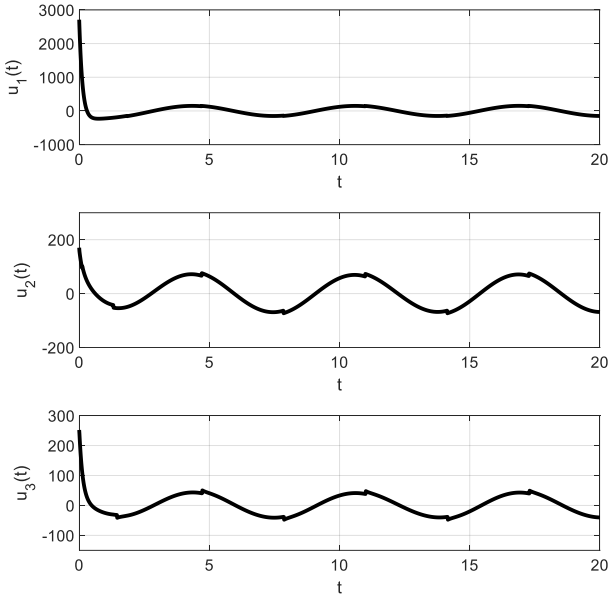


Fig.5. Trajectories of control signals.

Example 2: Rotational inverted pendulum

In this section, a rotational inverted pendulum is employed to investigate efficacy of proposed controller via Real-Time toolbox and MATLAB®/Simulink® software. In this case study, the suspended pendulum is stabilized in upright position [38]. The schematic view of rotational inverted pendulum and a picture of the practical system are displayed in Fig. 7, consisting of a rotational servo-motor driving the gear of output, rotational arm and suspended pendulum. In Fig. 7, the pendulum mass m_p , pendulum angle α_p , arm angle θ_a , pendulum length l_p , arm length r_a , inertia moment of effective mass J_b , control input u and motor torque τ_a are introduced. Dynamical equation of rotational inverted pendulum is formed as [39]

$$\begin{bmatrix} A_p + B_p \sin^2 \alpha_p & C_p \cos \alpha_p \\ C_p \cos \alpha_p & B_p \end{bmatrix} \begin{bmatrix} \ddot{\theta}_a \\ \ddot{\alpha}_p \end{bmatrix} + \begin{bmatrix} G_p \operatorname{sgn}(\dot{\theta}_a) + H_p \theta_a \\ -D_p \sin \alpha_p \end{bmatrix} + \begin{bmatrix} F_p + B_p (\sin 2 \alpha_p) \dot{\alpha}_p & -C_p (\sin \alpha_p) \dot{\alpha}_p \\ -0.5 B_p (\sin 2 \alpha_p) \dot{\theta}_a & E_p \end{bmatrix} \begin{bmatrix} \dot{\theta}_a \\ \dot{\alpha}_p \end{bmatrix} = \begin{bmatrix} I_p u \\ 0 \end{bmatrix} \quad (42)$$

where $A_p = m_p r_a^2 + J_b$, $B_p = \frac{1}{3} m_p l_p^2$, $C_p = \frac{1}{2} m_p r_a l_p$, $D_p = \frac{1}{2} m_p g l_p$; E_p is the pendulum damping constant, F_p is the arm damping coefficient, I_p represents the control coefficient, H_p denotes the elasticity constant and G_p is the arm Coulomb friction. The initial states are given as $[\alpha_p(0), \dot{\alpha}_p(0), \theta_a(0), \dot{\theta}_a(0)] = [\pi, -1, -4, 2]$. The constant parameters are given as $A_p = 3.291$, $B_p = 0.125$, $C_p = 0.237$, $D_p = 6.052$, $E_p = 0.0132$, $F_p = 14.283$, $G_p = 14.283$, $H_p = 1.72$, $I_p = 6.38$.

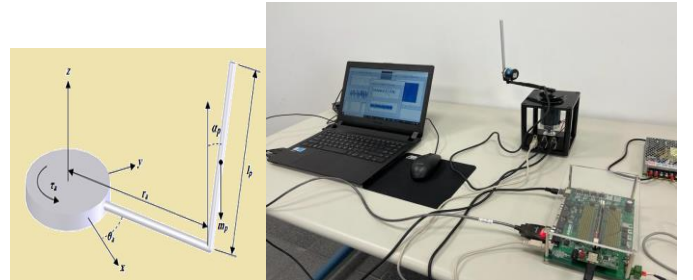


Fig. 7. Schematic view and apparatus of rotational inverted pendulum.

The simulations of the inverted pendulum system are represented in Figs. 8- 11. The angular position of the rotational pendulum tracks the desired trajectory $0.5\sin(t)$. From Fig.8, it can be displayed that the position and velocity of inverted pendulum suitably track the desired trajectories. Time history of the switching surface is demonstrated in Fig.9, which shows that the sliding variable converges to zero. Time response of control input is illustrated in Fig.10, which displays that the control signal has slight vibration and is robust to perturbations. Moreover, the time trajectory of the adaptation gain is exposed in Fig.11, where it demonstrates that the adaptation gain is a constant value and does not varies with time. Finally, simulation results on the rotational inverted pendulum system approve the effectiveness of the suggested technique.

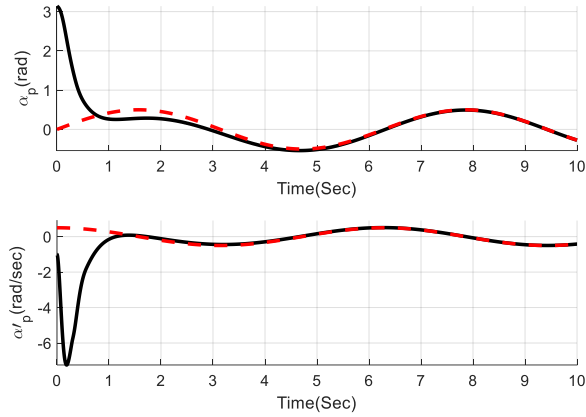


Fig.8. Time histories of pendulum's angular position and velocity.

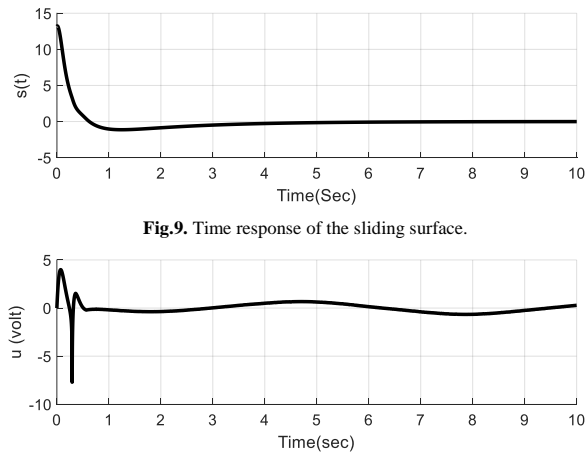


Fig.9. Time response of the sliding surface.

Fig.10. Time history of the control input

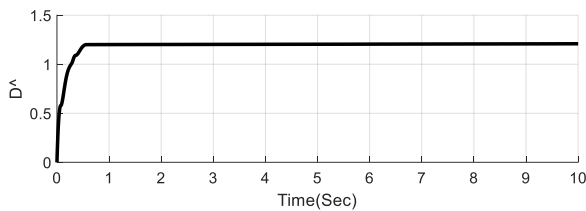


Fig.11. Adaptation gain

In this section, experimental results are done on the experimental inverted pendulum system which is developed by TeraSoft® company in Taiwan. The system components are demonstrated in Fig. 12. This system has a support package in MATLAB® as Embedded Coder

Toolbox which supports the Texas instruments C2000 Processors. After implementation of the proposed method on the rotational inverted pendulum system, the following experimental results are obtained. Time histories of the angular position and velocity of the inverted pendulum and arm are illustrated in Fig. 13 and Fig. 14, respectively. It is confirmed that the angular position of arm is stabilized near 0.9 radian. The pendulum angular position is converged to π . Also, in Fig. 15, the time trajectory of the applied voltage to the DC motor is demonstrated. This experimental result reveals the efficiency and success of the control scheme in practice.

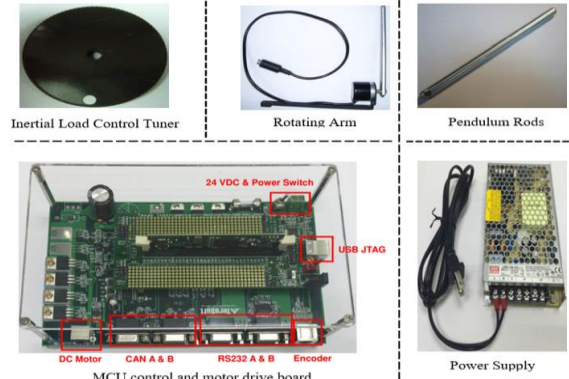


Fig. 12. Components of the practical apparatus.

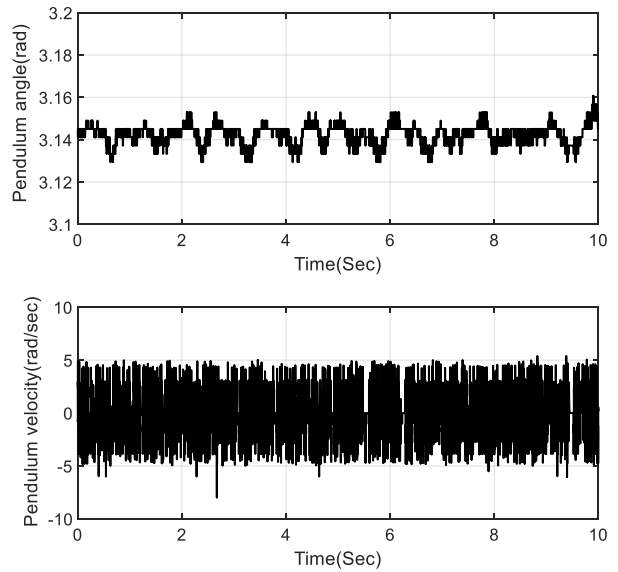


Fig. 13. Angular position and velocity of the pendulum.

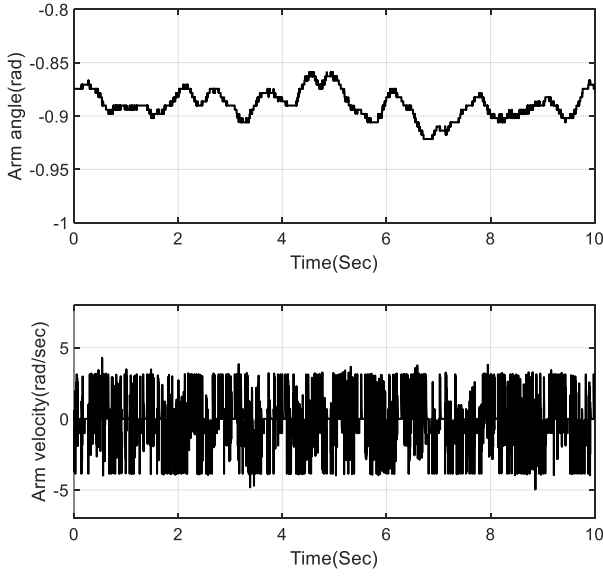


Fig. 14. Angular position and velocity of the arm.

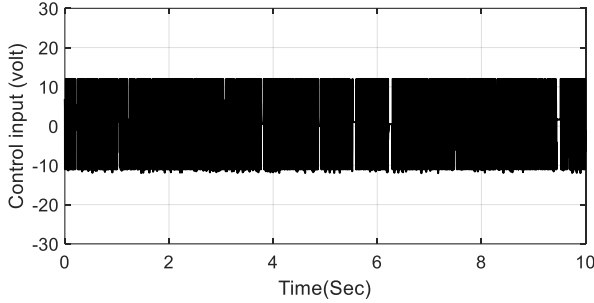


Fig. 15. Time response of the control signal.

V. CONCLUSIONS

In this article, a new method for finite-time stability of a robotic manipulator with nonlinear second-order equation was proposed. The suggested control method was derived from a new idea of Lyapunov candidate functional including an absolute function based on a fractional power of the sliding surface. The new scheme can eliminate discontinuity in the control laws, which is the principal disadvantage of SMC called chattering phenomenon. Furthermore, an adaptive control procedure was planned to estimate the unknown bound of external disturbance. Moreover, an extension of the recommended control procedure based on the barrier function adaptive TSMC is advised for better performance and robust tracking control of the perturbed nonlinear systems. Some simulation and experimental outcomes demonstrated efficiency of planned technique in avoiding the chattering problem as well as maintaining the robust performance. This novel concept of Lyapunov candidate functional can be combined with any classes of sliding mode techniques to form smooth and continuous controllers.

Appendix 1

The parameters on model are given by [40]

$$\begin{aligned}
 b_{11} = & I_{l_1} + m_{l_1} l_1^2 + k_{r_1}^2 I_{m_1} + I_{l_2} + m_{m_2} a_1^2 + I_{m_2} \\
 & + m_{l_2} (a_1^2 + l_2^2 + 2a_1 l_2 c_2) + I_{l_3} \\
 & + I_{m_3} + m_{m_3} (a_1^2 + a_2^2 + 2a_1 a_2 c_1) \\
 & + m_{l_3} (a_1^2 + a_2^2 + l_3^2 + 2a_1 a_2 c_2 + 2a_1 l_3 c_{23} + 2a_2 l_3 c_3),
 \end{aligned}$$

$$\begin{aligned}
 b_{22} = & I_{l_2} + I_{l_3} + k_{r_2}^2 I_{m_2} + I_{m_3} + m_{m_3} a_2^2 + m_{l_2} l_2^2 \\
 & + m_{l_3} (a_2^2 + l_3^2 + 2a_2 l_3 c_3),
 \end{aligned}$$

$$b_{33} = I_{l_3} + k_{r_3}^2 I_{m_3} + m_{l_3} l_3^2,$$

$$\begin{aligned}
 b_{12} = b_{21} = & I_{l_2} + I_{l_3} + k_{r_2} I_{m_2} + I_{m_3} + m_{m_3} (a_2^2 + a_1 a_2 c_2) \\
 & + m_{l_2} (l_2^2 + a_1 l_2 c_2) \\
 & + m_{l_3} (a_2^2 + l_3^2 + a_1 a_2 c_2 + a_1 l_3 c_{23} + 2a_2 l_3 c_3),
 \end{aligned}$$

$$b_{13} = b_{31} = I_{l_3} + k_{r_3} I_{m_3} + m_{l_3} (l_3^2 + a_1 l_3 c_{23} + a_2 l_3 c_3),$$

$$b_{23} = b_{32} = I_{l_3} + k_{r_3} I_{m_3} + m_{l_3} (l_3^2 + a_2 l_3 c_3),$$

$$\begin{aligned}
 h_{11} = & -m_{m_3} a_1 a_2 s_1 \dot{q}_1 \\
 & - (m_{l_2} + a_1 l_2 s_2 + m_{l_3} a_1 a_2 s_2 + m_{l_3} a_1 l_3 s_{23}) \dot{q}_2 \\
 & - (m_{l_3} a_1 l_3 s_{23} + m_{l_3} a_2 l_3 s_3) \dot{q}_3,
 \end{aligned}$$

$$h_{22} = -(m_{l_3} a_2 l_3 s_3) \dot{q}_3,$$

$$h_{33} = -(m_{l_3} a_1 a_2 s_2) \dot{q}_2 - (m_{l_3} a_2 l_3 s_3) \dot{q}_3,$$

$$\begin{aligned}
 h_{12} = & -(m_{l_2} a_1 l_2 s_2 + m_{l_3} a_1 a_2 s_2 + m_{l_3} a_1 l_3 s_{23}) \dot{q}_1 \\
 & - (m_{l_3} a_1 l_3 s_{23} + m_{l_3} a_2 l_3 s_3) \dot{q}_3 \\
 & - (m_{l_3} a_1 a_2 s_2 + m_{l_3} a_1 l_3 s_{23} + m_{m_3} a_1 a_2 s_2 + m_{l_2} a_1 l_2 s_2) \dot{q}_2,
 \end{aligned}$$

$$\begin{aligned}
 h_{13} = & -(m_{l_3} a_1 l_3 s_{23} + m_{l_3} a_2 l_3 s_3) \dot{q}_1 \\
 & - (m_{l_3} a_1 l_3 s_{23} + m_{l_3} a_2 l_3 s_3) \dot{q}_2 \\
 & - (m_{l_3} a_2 l_3 s_2 + m_{l_3} a_1 l_3 s_{23}) \dot{q}_3,
 \end{aligned}$$

$$h_{21} = (m_{l_2} a_1 l_2 s_2 + m_{l_3} a_1 a_2 s_2 + m_{l_3} a_1 l_3 s_{23}) \dot{q}_1 - (m_{l_3} a_2 l_3 s_3) \dot{q}_3,$$

$$h_{23} = -(m_{l_3} a_2 l_3 s_3) \dot{q}_1 - (m_{l_3} a_2 l_3 s_3) \dot{q}_2 - (m_{l_3} a_2 l_3 s_3) \dot{q}_3,$$

$$h_{31} = (m_{l_3} a_1 l_3 s_{23} + m_{l_3} a_2 l_3 s_3) \dot{q}_1 + (m_{l_3} a_2 l_3 s_3) \dot{q}_2,$$

$$h_{32} = (m_{l_3} a_2 l_3 s_3) \dot{q}_1 + (m_{l_3} a_2 l_3 s_3) \dot{q}_2 - (m_{l_3} a_2 l_3 s_3) \dot{q}_3,$$

$$\begin{aligned}
 g_1(q) = & (m_{l_1} I_1 + m_{l_2} a_1 + m_{m_2} a_1 + m_{l_3} a_1 + m_{m_3} a_1) g c_1 \\
 & + (m_{l_2} I_2 + m_{l_3} a_2 + m_{m_3} a_2) g c_{12} + m_{l_3} l_3 g c_{123},
 \end{aligned}$$

$$g_2(q) = (m_{l_2} l_2 + m_{l_3} a_2 + m_{m_3} a_2) g c_{12} + m_{l_3} l_3 g c_{123},$$

$$g_3(q) = m_{l_3} l_3 g c_{123},$$

with $c_1 = \cos q_1$, $s_1 = \sin q_1$, $c_2 = \cos q_2$, $s_2 = \sin q_2$, $c_3 = \cos q_3$, $c_{12} = \cos(q_1 + q_2)$, $c_{123} = \cos(q_1 + q_2 + q_3)$, $s_{12} = \sin(q_1 + q_2)$ and $s_{123} = \sin(q_1 + q_2 + q_3)$.

REFERENCES

- [1] J. Wang, T. Ru, J. Xia, H. Shen, and V. Sreeram, "Asynchronous Event-Triggered Sliding Mode Control for Semi-Markov Jump Systems Within a Finite-Time Interval," *IEEE Transactions on Circuits and Systems I: Regular Papers*, vol. 68, no. 1, pp. 458-468, 2021.
- [2] X. Zhang, W. Huang, and Q.-G. Wang, "Robust H_∞ Adaptive Sliding Mode Fault Tolerant Control for TS Fuzzy Fractional Order Systems With Mismatched Disturbances," *IEEE Transactions on Circuits and Systems I: Regular Papers*, vol. 68, no. 3, pp. 1297-1307, 2021.
- [3] P. Chen, L. Yu, and D. Zhang, "Event-triggered sliding mode control of power systems with communication delay and sensor faults," *IEEE Transactions on Circuits and Systems I: Regular Papers*, vol. 68, no. 2, pp. 797-807, 2022.
- [4] J. Oliveira, P. M. Oliveira, J. Boaventura-Cunha, and T. Pinho, "Chaos-based grey wolf optimizer for higher order sliding mode position control of a robotic manipulator," *Nonlinear Dynamics*, vol. 90, no. 2, pp. 1353-1362, 2017.
- [5] Z. Ma and G. Sun, "Dual terminal sliding mode control design for rigid robotic manipulator," *Journal of the Franklin Institute*, 2017.
- [6] A. Goel and A. Swarup, "MIMO Uncertain Nonlinear System Control via Adaptive High-Order Super Twisting Sliding Mode and its Application to

- Robotic Manipulator," *Journal of Control, Automation and Electrical Systems*, vol. 28, no. 1, pp. 36-49, 2017.
- [7] Y. Feng, M. Zhou, X. Zheng, F. Han, and X. Yu, "Full-Order Terminal Sliding-Mode Control of MIMO Systems with Unmatched Uncertainties," *Journal of the Franklin Institute*, 2017.
- [8] M. Ghasemi, S. G. Nersesov, and G. Clayton, "Finite-time tracking using sliding mode control," *Journal of the Franklin Institute*, vol. 351, no. 5, pp. 2966-2990, 2014.
- [9] X.-T. Tran and H.-J. Kang, "Adaptive hybrid high-order terminal sliding mode control of MIMO uncertain nonlinear systems and its application to robot manipulators," *International Journal of Precision Engineering and Manufacturing*, vol. 16, no. 2, pp. 255-266, 2015.
- [10] Y. Zhang, R. Li, T. Xue, Z. Liu, and Z. Yao, "An analysis of the stability and chattering reduction of high-order sliding mode tracking control for a hypersonic vehicle," *Information Sciences*, vol. 348, pp. 25-48, 2016.
- [11] I. M. Boiko, "Chattering in sliding mode control systems with boundary layer approximation of discontinuous control," *International Journal of Systems Science*, vol. 44, no. 6, pp. 1126-1133, 2013.
- [12] J. Yang, S. Li, and X. Yu, "Sliding-mode control for systems with mismatched uncertainties via a disturbance observer," *IEEE Transactions on Industrial Electronics*, vol. 60, no. 1, pp. 160-169, 2013.
- [13] J. Huang, L. Sun, Z. Han, and L. Liu, "Adaptive terminal sliding mode control for nonlinear differential inclusion systems with disturbance," *Nonlinear Dynamics*, vol. 72, no. 1-2, pp. 221-228, 2013.
- [14] S. Mondal and C. Mahanta, "Adaptive second order terminal sliding mode controller for robotic manipulators," *Journal of the Franklin Institute*, vol. 351, no. 4, pp. 2356-2377, 2014.
- [15] L. Zhao and Y. Jia, "Decentralized adaptive attitude synchronization control for spacecraft formation using nonsingular fast terminal sliding mode," *Nonlinear Dynamics*, vol. 78, no. 4, pp. 2779-2794, 2014.
- [16] S. Mobayen, "An adaptive fast terminal sliding mode control combined with global sliding mode scheme for tracking control of uncertain nonlinear third-order systems," *Nonlinear Dynamics*, vol. 82, no. 1-2, pp. 599-610, 2015.
- [17] W. Wang, Q. Zhao, Y. Zhao, and D. Du, "A nonsingular terminal sliding mode approach using adaptive disturbance observer for finite-time trajectory tracking of MEMS triaxial vibratory gyroscope," *Mathematical Problems in Engineering*, vol. 2015, 2015.
- [18] N. He, C. Jiang, B. Jiang, and Q. Gao, "Terminal sliding mode control with unidirectional auxiliary surfaces for hypersonic vehicles based on adaptive disturbance observer," *Mathematical Problems in Engineering*, vol. 2015, 2015.
- [19] S. He, D. Lin, and J. Wang, "Chattering-free adaptive fast convergent terminal sliding mode controllers for position tracking of robotic manipulators," *Proceedings of the Institution of Mechanical Engineers, Part C: Journal of Mechanical Engineering Science*, vol. 230, no. 4, pp. 514-526, 2016.
- [20] Q. Zhang, H. Liu, C. Wang, and Y. Li, "Robust adaptive terminal control for near space vehicle based on second order sliding mode disturbance observer," in *Control Conference (CCC), 2016 35th Chinese*, 2016, pp. 591-595: IEEE.
- [21] S. Lyu, Z. H. Zhu, S. Tang, and X. Yan, "Fast Nonsingular Terminal Sliding Mode to Attenuate the Chattering for Missile Interception with Finite Time Convergence," *IFAC-PapersOnLine*, vol. 49, no. 17, pp. 34-39, 2016.
- [22] W. Wang and X. Yu, "Chattering free and nonsingular terminal sliding mode control for attitude tracking of a quadrotor," in *Control And Decision Conference (CCDC), 2017 29th Chinese*, 2017, pp. 719-723: IEEE.
- [23] Y.-j. Wu, J.-x. Zuo, and L.-h. Sun, "Adaptive terminal sliding mode control for hypersonic flight vehicles with strictly lower convex function based nonlinear disturbance observer," *ISA transactions*, vol. 71, pp. 215-226, 2017.
- [24] D. Xu, Q. Liu, W. Yan, and W. Yang, "Adaptive Terminal Sliding Mode Control for Hybrid Energy Storage Systems of Fuel Cell, Battery and Supercapacitor," *Ieee Access*, vol. 7, pp. 29295-29303, 2019.
- [25] B. An, B. Wang, Y. Wang, and L. Liu, "Adaptive Terminal Sliding Mode Control for Reentry Vehicle Based on Nonlinear Disturbance Observer," *IEEE Access*, vol. 7, pp. 154502-154514, 2019.
- [26] S. Ahmed, H. Wang, and Y. Tian, "Adaptive high-order terminal sliding mode control based on time delay estimation for the robotic manipulators with backlash hysteresis," *IEEE Transactions on Systems, Man, and Cybernetics: Systems*, 2019.
- [27] Y. Wang, J. Chen, F. Yan, K. Zhu, and B. Chen, "Adaptive super-twisting fractional-order nonsingular terminal sliding mode control of cable-driven manipulators," *ISA transactions*, vol. 86, pp. 163-180, 2019.
- [28] Y. Wang, B. Li, F. Yan, and B. Chen, "Practical adaptive fractional-order nonsingular terminal sliding mode control for a cable-driven manipulator," *International Journal of Robust and Nonlinear Control*, vol. 29, no. 5, pp. 1396-1417, 2019.
- [29] U. Ansari, A. H. Bajodah, and M. T. Hamayun, "Quadrotor control via robust generalized dynamic inversion and adaptive non-singular terminal sliding mode," *Asian Journal of Control*, vol. 21, no. 3, pp. 1237-1249, 2019.
- [30] X. Liu, S. Qi, R. Malekain, and Z. Li, "Observer-based composite adaptive dynamic terminal sliding-mode controller for nonlinear uncertain SISO systems," *International Journal of Control, Automation and Systems*, vol. 17, no. 1, pp. 94-106, 2019.
- [31] Y. Wang, K. Zhu, F. Yan, and B. Chen, "Adaptive super-twisting nonsingular fast terminal sliding mode control for cable-driven manipulators using time-delay estimation," *Advances in Engineering Software*, vol. 128, pp. 113-124, 2019.
- [32] J. Keighobadi, M. Hosseini-Pishrobat, and J. Faraji, "Adaptive neural dynamic surface control of mechanical systems using integral terminal sliding mode," *Neurocomputing*, vol. 379, pp. 141-151, 2020.
- [33] K. Elikor and W. Zhang, "Finite-time Adaptive Integral Backstepping Fast Terminal Sliding Mode Control Application on Quadrotor UAV," *International Journal of Control, Automation and Systems*, vol. 18, no. 2, pp. 415-430, 2020.
- [34] J. A. Moreno, D. Y. Negrete, V. Torres-González, and L. Fridman, "Adaptive continuous twisting algorithm," *International Journal of Control*, vol. 89, no. 9, pp. 1798-1806, 2016.
- [35] T. Sanchez, J. A. Moreno, and L. M. Fridman, "Output feedback continuous twisting algorithm," *Automatica*, vol. 96, pp. 298-305, 2018.
- [36] A. Chalanga, S. Kamal, and B. Bandyopadhyay, "Continuous integral sliding mode control: A chattering free approach," in *2013 IEEE International Symposium on Industrial Electronics*, 2013, pp. 1-6: IEEE.
- [37] C. Xiu and P. Guo, "Global terminal sliding mode control with the quick reaching law and its application," *IEEE Access*, vol. 6, pp. 49793-49800, 2018.
- [38] O. Boubaker, "The inverted pendulum benchmark in nonlinear control theory: a survey," *International Journal of Advanced Robotic Systems*, vol. 10, no. 5, p. 233, 2013.
- [39] I. Hassanzadeh and S. Mobayen, "Controller design for rotary inverted pendulum system using evolutionary algorithms," *Mathematical Problems in Engineering*, vol. 2011, no. Article ID 572424, p. 17 Pages, 2011.
- [40] S. Mobayen, F. Tchier, and L. Ragoub, "Design of an adaptive tracker for n-link rigid robotic manipulators based on super-twisting global nonlinear sliding mode control," *International Journal of Systems Science*, pp. 1-13, 2017.